Lattice dynamics study of zigzag and armchair carbon nanotubes

A. Charlier
Laboratoire de Physique du Solide, 1 Boulevard Arago, 57078 Metz Cedex 03, France

E. McRae
Laboratoire de Chimie du Solide Minéral (URA 158), Boîte Postale 239, 54506 Vandoeuvre les Nancy, France

M.-F. Charlier, A. Spire, and S. Forster
Laboratoire de Physique du Solide, 1 Boulevard Arago, 57078 Metz Cedex 03, France
(Received 16 July 1997; revised manuscript received 13 November 1997)

We propose a very simple model of lattice dynamics of carbon nanotubes. Using a De Launay model, the atomic force constants and phonon density of states are given as functions of the nanotube radius. Elastic constants, a Young modulus, and Poisson ratio are derived from phonon dispersion curves for a homogeneous deformation. [S0163-1829(98)00911-4]

I. INTRODUCTION

Immediately following the discovery of carbon nanotubes by Iijima[1] in 1991, intense activity was undertaken in both experimental and theoretical fields.[2–5] The electronic properties of such one-dimensional (1D) carbon nanotubes are seen to arise predominantly from intralayer interactions rather than from interlayer interactions between multilayers within coaxially nested carbon nanotubes or between two different nanotubes. The symmetry of a single nanotube plays an essential role in understanding the basic underlying physics. In this work, we will focus on the properties of single layer (single wall) nanotubes, designated SWT's. Such a SWT is an ideal substance to study because its simple structure is defined unambiguously by its diameter, length, and chirality, and its size-specific properties are analyzed on the basis of a single sheet of graphite called ''graphene.''[6–11] Theoretically[2,3,9,11–13] a nanotube is predicted to be a semiconductor or a metal depending on its diameter and chirality. This arises from the fact that the translational symmetry in graphene, persists along the tube axis but no longer exists around its circumference. Thus the wave vectors of both electrons and phonons possess continuous values along the direction corresponding to the tube axis in the Brillouin zone but can take only sets of discrete values around the circumference. This size-dependent zone folding effect is the salient feature of nanotubes that governs their basic properties.

Since 1993, several publications[14–18] have dealt with the vibrational (Raman) spectra of multiwalled carbon nanotubes (MWT's). More recent works[19–22] have treated SWT's and the data have been reviewed in Refs. 10,23. Along with the experimental investigations, a number of authors have also treated the theoretical aspects of SWT's relating to the symmetry-dependent number of modes and the diameter-dependent frequencies.[10,19,21–25] Experimental first-order Raman-active vibrational mode frequencies have been proposed[20] for a series of armchair (N_x,N_x) nanotubes for $x=8,9,10,11$ and satisfactory agreement between the theoretical model and the experimental values is found only for the highest frequencies.

The present work aims to improve agreement between theory and experiment. To do so, we will use first the deformation potential introduced in Refs. 26,27 which is associated with the conformal mapping of a graphene plane to form a cylindrical tube and secondly, the De Launay model[28,29] to study the dynamical properties of zigzag and armchair carbon nanotubes. Indeed, the experimentally observed multiple splitting of the Raman peaks[21,22] may be understood in terms of the phonon dispersion relation of graphene. The discrete allowed wave vectors around the tubule circumference mean that the optical phonons of these wave vectors can be excited with their energies given by the dispersion relation of graphene at the same wave vector provided that the dispersion remains unchanged by rolling into a closed tube.[12,13]

In what follows, we will first briefly review the notation used in defining the nanotube structures. In Sec. III we then successively present the model used in our evaluations, the resulting dispersion relations, and finally the specific heat, Debye temperatures, and elastic constants. Calculational details have been put into the appendixes.

II. NANOTUBE STRUCTURES

We use the notation of Refs. 6 and 11 in which a tubule is defined in terms of the two direct lattice vectors $\mathbf{a}_1$ and $\mathbf{a}_2$ of a 2D graphene sheet and a pair of integers (n,m). For the zigzag tubule $m=0$ and for the armchair $n=m$ (Fig. 1). The widely used model of a SWT consists of rolling up a semi-infinite graphene sheet into a cylindrical tube of constant

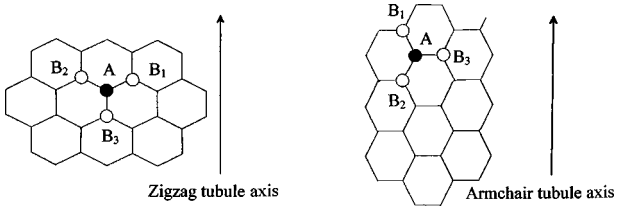

FIG. 1. Representation of armchair and zigzag tubules. Atoms B_1, B_2, and B_3 are the first nearest neighbors of atom A.

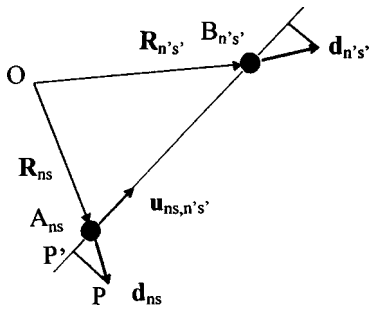

FIG. 2. Central and angular forces. $\mathbf{u}_{nsn's'}$ is the unit vector in the direction of the line joining the atoms in the equilibrium positions defined by $\mathbf{R}_{ns}$ and $\mathbf{R}_{n's'}$; $\mathbf{d}_{ns}$ and $\mathbf{d}_{n's'}$ represent the instantaneous displacements, which can be decomposed into radial ($\mathbf{A}_{ns}\mathbf{P}'$) and angular ($\mathbf{P}'\mathbf{P}$) components.

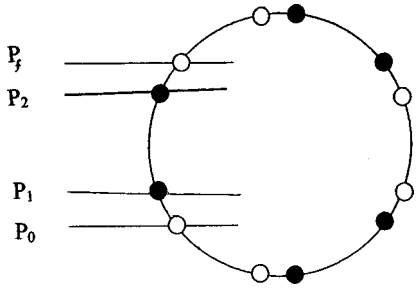

FIG. 3. Example of a (6,6) armchair nanotube. Filled and unfilled circles represent atoms in two different planes perpendicular to the tube axis. Planes P_0 to P_2 and P_f are parallel to tube axis. Interactions between planes P_0 and P_f are ''further'' interactions, where P_f symbolizes all planes beyond P_1 and P_2.

radius. To this conformal mapping corresponds a simple deformation potential[26,27] taking into account the effects of curvature on the one-dimensional electronic properties[26] of carbon nanotubes.

In a graphene sheet the carbon atoms are placed in the vertices of open hexagons, the edges of which have a length of $d_{\text{C-C}}=1.42$,Å (the smallest distance between atoms within the graphitic plane). The vectors of the primitive cell in the $(\mathbf{e}_1,\mathbf{e}_2,\mathbf{e}_3)$ orthonormal basis for graphite are

$$\mathbf{a}_1=\begin{pmatrix} a \\ 0 \\ 0 \end{pmatrix},\quad \mathbf{a}_2=\begin{pmatrix} -a/2 \\ a\sqrt{3}/2 \\ 0 \end{pmatrix},\quad \mathbf{a}_3=\begin{pmatrix} 0 \\ 0 \\ c \end{pmatrix}, \tag{2.1}$$

with $\|\mathbf{a}_1\|=\|\mathbf{a}_2\|=a=\sqrt{3}d_{\text{C-C}}=2.46$ Å, $\|\mathbf{a}_3\|=c=2d_{p-p}=6.70$ Å; d_{p-p} is the distance between two graphitic planes. From these equations, we can immediately determine the vectors of the reciprocal lattice:

$$\mathbf{b}_1=\begin{pmatrix} 2\pi/a \\ 2\pi/\sqrt{3}a \\ 0 \end{pmatrix},\quad \mathbf{b}_2=\begin{pmatrix} 0 \\ -4\pi/\sqrt{3}a \\ 0 \end{pmatrix},\quad \mathbf{b}_3=\begin{pmatrix} 0 \\ 0 \\ 2\pi/c \end{pmatrix}. \tag{2.2}$$

For graphene $\mathbf{a}_3=\mathbf{b}_3=\mathbf{0}$. In discussing the symmetry of the carbon nanotubes, it is assumed that the tubule length is much greater than its diameter so that the contributions of the end caps (if any exist) can be neglected in treating the physical properties. The symmetry groups are symmorphic for armchair and zigzag nanotubes where the translational and rotation symmetry operations can be executed independently.[6,10,30]

III. DYNAMICAL STUDY OF CARBON NANOTUBES

The De Launay model[28] assumes that there exist two forces between pairs of atoms: a central or radial force which depends only on the distance between the two atoms and an angular force which depends only on the angle between the line joining two atoms at any given instant and the line between the same two atoms at equilibrium: see Fig. 2. A crystal lattice made up of N atoms in the primitive cell is considered as the sum of N sublattices. Each sublattice is taken to possess the symmetry of the whole crystal. We take into account the interactions between atoms in the same sublattice as well as those between different sublattices. We will utilize the following notation: $\alpha_{v,i}(\alpha'_{v,i})$ is the atomic force constant corresponding to the central forces (angular forces); the index v specifies whether the atoms are first, second, third, . . . , nearest neighbors and i corresponds to an interaction with the atoms within the same plane if $i=$intra and with the atoms in (first, second, . . .) nearest planes if $i=$inter. Satisfactory results are obtained for graphite using the five force constants $\alpha_{1,\text{intra}}$, $\alpha'_{1,\text{intra}}$, $\alpha_{2,\text{intra}}$, $\alpha_{1,\text{inter}}$, and $\alpha'_{1,\text{inter}}$.

In the case of single-walled nanotubes, such a distinction between ''intraplanar'' and ''interplanar'' is somewhat arbitrary and consideration can be limited to first-, second-, and further-neighbor interactions characterized respectively by atomic force constants $\alpha_1,\alpha_2,\alpha_f,(\alpha'_1,\alpha'_2,\alpha'_f)$ for central (angular) forces. Let us take, as an example, the (6,6) armchair tube of Fig. 3. We consider the various atoms to be on planes P_0, P_1, and P_2, P_0 being the reference plane. First- and second-nearest-neighbor interactions correspond to those between P_0, P_1, and P_2, respectively, and ''further'' interactions to those between planes P_0 and P_f comprising all the more distant planes. This reasoning implies that the values of the atomic force constants $\alpha_{1,\text{inter}}$ and $\alpha'_{1,\text{inter}}$ used for graphite must be increased in the case of the nanotubes, since the distance P_0-P_f is less than the interplanar distance in graphite. Furthermore, Fig. 3 shows that depending on the tube diameter, it might be necessary to take into account more planes beyond P_2. However, in our case, the modified values of $\alpha_{1,\text{inter}}$ and $\alpha'_{1,\text{inter}}$ denoted α_f and α'_f integrate the overall effects of all atomic planes superior to second neighbors. The above remarks imply that we must introduce a new force constant α'_2. Indeed the radial force constant α_2 remains almost unmodified under conformal mapping, but the angular force constant α'_2 between second nearest neighbors cannot be neglected because of the nanotube curvature.

The operation of transforming a graphene sheet into a tube can be understood as adding to the graphene Hamiltonian a deformation potential energy term attributed to the alignment defects of the σ orbitals due to curvature (i.e., nonplanarity) of the graphene plane. As in Ref. 27 and as observed on Fig. 1, the bond AB_3 remains parallel to the tubule axis and consequently is not deformed for zigzag tubules. In the case of armchair tubules the σ_{AB_3} bond is the

TABLE I. Atomic force constants: $\alpha_v(\alpha'_v)$ is the atomic force constant corresponding to the central (angular) forces; the index v specifies first, second or ''further'' neighbor interactions. For graphite, α_f and α'_f correpond to $\alpha_{1,\text{inter}}$ and $\alpha'_{1,\text{inter}}$.

	α_1	α'_1	α_2	α'_2	α_f	α'_f	β_1	β_3
Graphite[29]	505.1	84.4	73.7		5.9	0.72		
(N_x,N_x)	505.1	87.8	73.7	15.0	68.0	11.0	$4.4/N_x$	$8.8/N_x$
$(N_y,0)$	505.1	87.8	73.7	15.0	68.0		$37.5/N_y$	

most deformed by rolling up a graphene sheet. Deforming the flat graphene sheet to form a tubule means that in addition to the initial interatomic force constants we should now add supplementary terms β_i.

(i) for the zigzag tubules and for the $A\leftrightarrow B$ interactions, only the atoms denoted B_1 and B_2 are concerned (cf. Fig. 1):

$$\beta_{AB_1}^{\text{zigzag}}=\beta_{AB_2}^{\text{zigzag}}=\beta_1,\quad \beta_{AB_3}^{\text{zigzag}}=0. \tag{3.1}$$

(ii) for the armchair tubules, the three atoms B_1, B_2, and B_3 intervene (cf. Fig. 1):

$$\beta_{AB_1}^{\text{armchair}}=\beta_{AB_2}^{\text{armchair}}=\beta_1,\quad \beta_{AB_3}^{\text{armchair}}=\beta_3. \tag{3.2}$$

Since the alignment defect decreases as the radius increases we take β_1 and β_3 proportional to the inverse radius of the tubules; we recall that $R^{\text{zigzag}}=\sqrt{3}N_y d_{\text{C-C}}/2\pi$ and $R^{\text{armchair}}=3N_x d_{\text{C-C}}/2\pi$.

Account is taken of the orbital alignment defects for the zigzag tubules for atoms B_1 or B_2 by replacing $\alpha'_{1,\text{intra}}$ in the dynamic matrix of graphite by $\alpha'_1+\beta_1$ (see Appendix A); for the armchair tubes, for atom B_1 or B_2: $\alpha'_{1,\text{intra}}\rightarrow\alpha'_1+\beta_1$ and for atom B_3: $\alpha'_{1,\text{intra}}\rightarrow\alpha'_1+\beta_3$. We recall that $\alpha_{1,\text{inter}}\rightarrow\alpha_f$ and $\alpha'_{1,\text{inter}}\rightarrow\alpha'_f$.

By taking into account the new force constants β_1, β_3, and α'_2 the dynamical matrix of graphite is transformed into a dynamical matrix of the nanotube. The numerical values of the constants α_i, α'_i, and β_i (Table I) are determined by adjusting their values in the dynamical matrix so as to obtain the best fits of calculated and observed Raman frequencies for the different tubule radii corresponding to $N_x=8$, 9, 10, and 11. Comparison of the frequencies is given in Table II ($1\,\text{THz}=33.35\ \text{cm}^{-1}$).

It is of interest to compare the frequencies in Table II with those force constants with which they are associated in the dynamical matrix. As concerns the low frequencies (3.47 and 5.57 THz) and to a lesser extent 11.3 THz they are strongly dependent on α_f and α'_f which signifies that these frequencies are characteristic of the ''further'' atom interactions beyond second-order neighboring interactions. We may observe on all spectra ($N_x=5,200$) the frequency at 3.47 THz indicated as characteristic of nanotubes.[16] The frequency close to 25 THz is linked to the force constant α'_f which characterizes the angular forces between first neighbors; this frequency, characteristic of graphite is slightly shifted because of the interactions due to the alignment defects. The high frequencies (47.75 and 48.23 THz) are due to first and second neighbor interactions: they are thus also observed on graphite, although slightly modified in the case of the nanotubes due to the angular distortion.

TABLE II. Experimental and theoretical Raman frequencies in THz for armchair nanotubes. The left hand column shows experimentally observed frequencies for a powder containing (8,8), (9,9), (10,10), and (11,11) nanotubes. The right hand column gives our calculated values.

Experimental ν (Ref. 20)	Theoretical ν
3.47	3.47
5.57	5.57
11.30	11.30
20.17	19.16
22.63	22.64
25.63	25.63
40.38	39.58
45.74	43.24
46.46	43.24
46.97	46.96
47.75	47.30
48.23	48.08

Let us now examine the passage from graphene to graphite. We recall that experimentally, an isolated plane of graphene has never been observed. But SWT's have been synthesized in many laboratories and these nanotubes in the limit of high values of radii must be equivalent to graphene. In graphite the interplanar interactions are weak but necessary for the stability of the crystal. We observe from Fig. 3 that the interactions classified in nanotubes as ''further'' atom interactions are equivalent to graphene's third, fourth, etc., interplanar interactions. If we increase the tubule's radius the distance d in Fig. 3 goes to infinity and the tubule becomes a graphene sheet. We lose the interactions between atoms symmetric with respect to the center of the circle and separated by the distance d. In this limit, there is no equivalent to interplanar interactions existing in graphite. We deduce from this that graphene is unstable due to lack of interlayer coupling. This means also that a sheet comprising two graphene planes might exist if the interplanar forces were sufficiently strong. This explains why for SWT's the force constants α_f and α'_f must be much greater than in the case of graphite ($\alpha_{1,\text{inter}}$ and $\alpha'_{1,\text{inter}}$) and that the force constants corresponding to first- and second-neighbor interactions α_1, α'_1, and α_2 are almost unchanged. We now turn to the phonon density of states.

The phonon density was calculated using a method based on counting the number of eigenfrequencies existing in each interval between ν and $\nu+d\nu$; the phonon density is obtained by diagonalizing many times the dynamical matrix for points of the first Brillouin zone;[31] Fig. 4 compares the density of states (DOS) for graphite, a (10,0) zigzag, and a (10,10) armchair nanotube. The graphitic character of the nanotubes stands out.

Using the density of states $g(\nu)$, and the Debye model for the specific heat in the form of a discrete sum over the frequencies:

$$C_v=\sum_\nu k_b\left(\frac{h\nu}{k_BT}\right)^2\frac{e^{h\nu/k_BT}g(\nu)}{(e^{h\nu/k_BT}-1)^2} \tag{3.3}$$

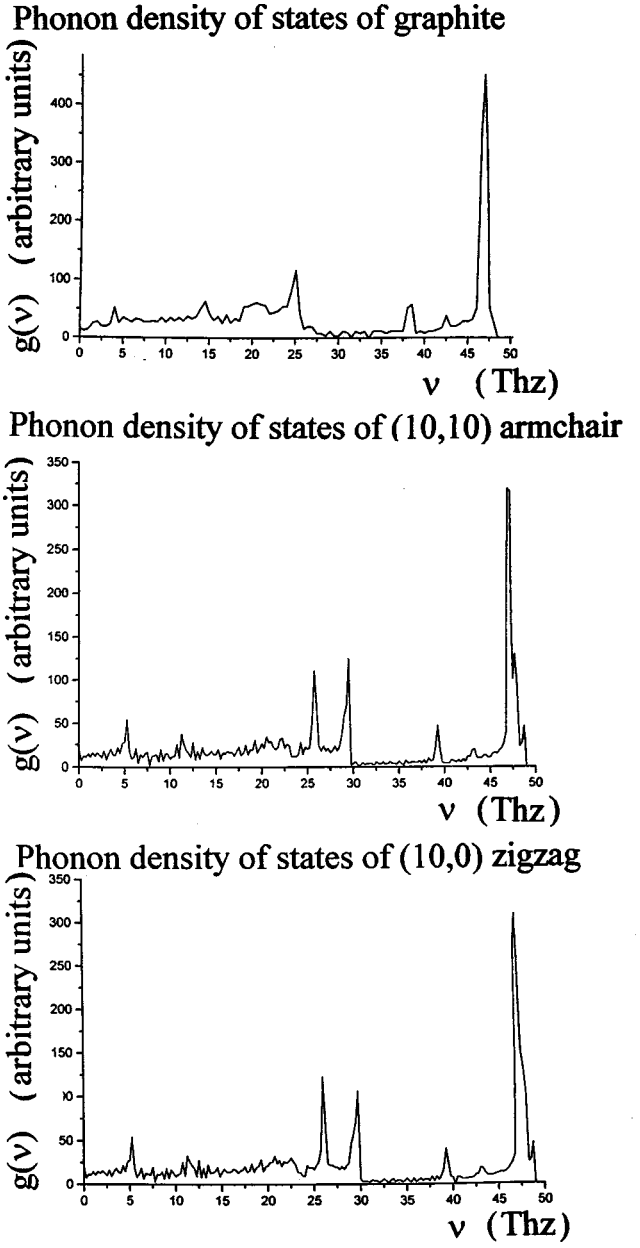

FIG. 4. Density of states of (10,10) armchair, (10,0) zigzag nanotubes compared to graphite.

one finds, at low temperatures,

$$C_v = \gamma T^3 + \alpha T, \tag{3.4}$$

where γT^3 and αT are the lattice and electronic contributions, respectively, with

$$\gamma = \frac{12\pi^4}{5} N k_B \left(\frac{1}{\Theta_D^3} \right). \tag{3.5}$$

k_B is the Boltzmann constant and Θ_D the Debye temperature. The results obtained using the De Launay model for graphite are close to those of the literature:[32–34] $\gamma = 2.7 \times 10^{-5}$ J mol^{-1} K^{-4} and $\Theta_D = 413$ K. For a (10,10) armchair tubule, $\gamma = 1.43 \times 10^{-5}$ J mol^{-1} K^{-4} and $\Theta_D = 475$ K and for a (10,0) zigzag tubule, $\gamma = 8.1 \times 10^{-6}$ J mol^{-1} K^{-4} and $\Theta_D = 621$ K. These values differ little for N_x comprised between 8 and 11.

We show in Appendix B the importance for carbon nanotubes of the elastic constants C_{11} and C_{66}; they allow the determination of C_{12}. For the evaluation of C_{11}, for example, we consider an acoustic branch of the phonon dispersion curves $\nu = \nu(k)$ which is almost linear in the neighborhood of $k = 0$. We consider the slope at the origin $p = \nu/k$ and we apply the relationship of Appendix B:

$$C_{11[100]} = \rho \frac{\omega_L^2}{k_1^2} = 10.25 \times 10^7 \left(\frac{\nu}{k} \right)^2, \tag{3.6}$$

where ν is in THz and k is dimensionless.

We recall[35] that λ and μ are the Lamé coefficients. The compression modulus K is given by $K = \lambda + (2/3)\mu$ with $\lambda = C_{12}$ and $\mu = (C_{11} + 2C_{12})/2$, so that $K = (C_{11} + 2C_{12})/3$. For a homogeneous deformation, the Young's modulus E_{Young} and Poisson's ratio σ_{Poisson} are defined by

$$E_{\text{Young}} = \frac{9K\mu}{3K + \mu} = \frac{(C_{11} + 2C_{12})(C_{11} - C_{12})}{(C_{11} + C_{12})}, \tag{3.7}$$

$$\sigma_{\text{Poisson}} = \frac{1}{2} \frac{3K - 2\mu}{3K + \mu} = \frac{C_{12}}{3(C_{11} + C_{12})}. \tag{3.8}$$

For the (10,10) tube, $C_{11} = 84.45 \times 10^{10}$ nm^2, $C_{12} = -13.89 \times 10^{10}$ nm^2, $E_{\text{Young}} = 789.8$ GPa. and $\sigma_{\text{Poisson}} = 0.065$. The Young's modulus is slightly size dependent rising with the diameter (for graphite $E_{\text{Young}} = 1020$ GPa).

IV. CONCLUSIONS

Our simple dynamical model using only six atomic force constants has been shown to yield quite satisfactorily those frequencies experimentally observed in Raman scattering studies of single wall carbon nanotubes[20] and to be in good agreement with results predicted theoretically for the armchair and zigzag tubes with diameters of the order of 10 to 15 Å.[13,21,24] Of particular interest is the fact that our model has allowed showing that a given atomic force constant may play a prominent role in determining a given observed Raman-active frequency.

It is of interest to examine the passage from graphene to graphite: (i) experimentally, an isolated plane of graphene has never been observed; (ii) a sheet comprising two graphene planes might exist if the interplanar forces were sufficiently strong; (iii) for an infinite number of parallel planes, i.e., the case of graphite, the interplanar forces become very weak.

We deduce from this that graphene is unstable due to lack of interlayer coupling, but that beyond a certain threshold, the greater the number of added graphene planes, the weaker the interplanar force constant between them. As a corollary, as we remove graphene planes from graphite, we increase the interplanar force constants.

Consider a coaxial, carbon multiwall tube from which we successively remove layers, starting from the outmost wall and finishing at a single walled tube. Upon the removal of each layer, the interlayer force constant increases to maintain the overall stability. This explains why, for SWT's, the ''interplanar'' force constants must be much greater than in the

case of graphite and that the intraplanar force constants are almost unchanged; this is clearly brought out in Table I.

APPENDIX A: DYNAMICAL MATRIX FOR CARBON NANOTUBES

In the frame of the De Launay model, application of the fundamental principle of dynamics leads to

$$m_s\ddot{\mathbf{d}}_{ns}=\sum_{n's'v}\mathbf{F}_{nsn's'v}=-m_s\omega_{ns}^2\mathbf{d}_{ns} \tag{A1}$$

with

$$\mathbf{F}_{nsn's'v}=-\alpha'_{v,i}(\mathbf{d}_{ns}-\mathbf{d}_{n's'})-(\alpha_{v,i}-\alpha'_{v,i})\times[\{\mathbf{u}_{nsn's'}\cdot(\mathbf{d}_{ns}-\mathbf{d}_{n's'})\}\mathbf{u}_{nsn's'}]. \tag{A2}$$

The index v indicates first, second, third, etc., neighbors under consideration. In the case of graphite the index i indicates whether the neighbor is within the same plane or in another. For single-walled carbon nanotubes the index i has no signification, the only distinction is between first-, second-, and further-neighbor interactions: $\alpha_{v,i}(\alpha'_{v,i})$ is replaced by $\alpha_v(\alpha'_v)$, $v=1,\ 2,\ f$ indicating first-, second-, or further-neighbor interactions.

A system of $3N$ equations in $3N$ unknowns is obtained, the unknowns being the components of the displacement vector:

$$m_s\ddot{d}_{nsj}-\sum_{n's'vj'}\{-\alpha'_{v,i}\delta_{jj'}+(\alpha'_{v,i}-\alpha_{v,i})\times u_{nsn's'j}u_{nsn's'j'}(d_{nsj'}-d_{n's'j'})\}=0 \tag{A3}$$

introducing

$$\mathbf{d}_{ns}=\mathbf{A}_{ns}e^{i(-\omega_{ns}t+\mathbf{k}\cdot\mathbf{R}_{ns})} \tag{A4}$$

we obtain for carbon nanotubes

$$-m_s\omega_{ns}^2A_{nsj}+\sum_{n's'vj'}\{-\alpha'_v\delta_{jj'}+(\alpha'_v-\alpha_v)\times u_{nsn's'j}u_{nsn's'j'}\}(A_{n's'j'}e^{i\mathbf{k}\cdot(\mathbf{R}_{n's'}-\mathbf{R}_{ns})}-A_{nsj'})=0. \tag{A5}$$

A nontrivial solution of this system of $3N$ equations exists for $|M(\mathbf{k})-m_s\omega_{ns}^2(\mathbf{k})I|=0$, where M is the dynamical matrix of the crystal and I the identity matrix.

In the case of hexagonal graphite, the primitive cell contains four independent carbon atoms denoted A, B, C, and D. Therefore we have four sublattices leading to a 12×12 dynamical matrix with 78 elements above the diagonal. This matrix adapted to carbon nanotubes has the form

$$\begin{pmatrix} A\leftrightarrow A & A\leftrightarrow B & A\leftrightarrow C & A\leftrightarrow D\\ B\leftrightarrow A & B\leftrightarrow B & B\leftrightarrow C & B\leftrightarrow D\\ C\leftrightarrow A & C\leftrightarrow B & C\leftrightarrow C & C\leftrightarrow D\\ D\leftrightarrow A & D\leftrightarrow B & D\leftrightarrow C & D\leftrightarrow D \end{pmatrix}, \tag{A6}$$

where $A\leftrightarrow B$, for example, expresses the interaction between the type A and B atoms. The dynamical matrix being Hermitian and the symmetry of the unit cell, lead to

$$\begin{pmatrix} A & B^* & C & 0\\ B & D & 0 & 0\\ C & 0 & A & B\\ 0 & 0 & B^* & D \end{pmatrix}; \tag{A7}$$

A, B, C, D, and 0 are 3×3 matrices.

The element of the dynamical matrix being

$$\sum_{n's'vj'}\{-\alpha'_v\delta_{jj'}+(\alpha'_v-\alpha_v)\times u_{nsn's'j}u_{nsn's'j'}\}(A_{n's'j'}e^{i\mathbf{k}\cdot(\mathbf{R}_{n's'}-\mathbf{R}_{ns})}-A_{nsj'}) \tag{A8}$$

we have explicitly

$$A_{11}(\mathbf{k})=\frac{3}{2}(\alpha_1+\alpha'_1)+2\alpha'_f+3\alpha_2\left\{1-\frac{1}{2}[\cos(2\pi k_1)+\cos2\pi(k_1+k_2)]\right\}+\frac{3}{4}(\beta_1+\beta_3)+\alpha'_2\left\{3-\frac{1}{2}[\cos2\pi k_1+\cos2\pi(k_1+k_2)]\right\}-2\cos(2\pi k_2),$$

$$A_{12}(\mathbf{k})=A_{21}(\mathbf{k})=-(\sqrt{3}/2)\alpha_2[\cos2\pi(k_1+k_2)-\cos(2\pi k_1)]+\frac{\sqrt{3}}{4}(\beta_1-\beta_3),$$

$$A_{13}(\mathbf{k})=A_{31}(\mathbf{k})=0,$$

$$A_{22}(\mathbf{k})=\frac{3}{2}(\alpha_1+\alpha'_1)+2\alpha'_f+3\alpha_2\left\{1-\frac{2}{3}\cos(2\pi k_2)-\frac{1}{6}[\cos(2\pi k_1)+\cos2\pi(k_1+k_2)]\right\}+\frac{5}{4}\beta_1+\frac{1}{4}\beta_3+\alpha'_2\left\{3-\frac{3}{2}[\cos2\pi k_1+\cos2\pi(k_1+k_2)]\right\},$$

$$A_{23}(\mathbf{k})=A_{32}(\mathbf{k})=0,$$

$$A_{33}(\mathbf{k}) = 3\alpha_1' + 2\alpha_f + 2\beta_1 + \beta_3 + \alpha_2'\{6 - 2[\cos 2\pi k_1 + \cos 2\pi(k_1+k_2) + \cos 2\pi k_2]\},$$

$$B_{11}(\mathbf{k}) = -\frac{1}{4}(\alpha_1 + 3\alpha_1')(e^{-2\pi i/3(k_1+2k_2)} + e^{-2\pi i/3(k_1-k_2)}) - \alpha_1 e^{2\pi i/3(2k_1+k_2)} - \frac{3}{4}\beta_1 e^{-2\pi i/3(k_1-k_2)} - \frac{3}{4}\beta_3 e^{-2\pi i/3(k_1+2k_2)},$$

$$B_{12}(\mathbf{k}) = B_{21}(\mathbf{k}) = \frac{\sqrt{3}}{4}(\alpha_1 - \alpha_1')(e^{-2\pi i/3(k_1-k_2)} - e^{-2\pi i/3(k_1+2k_2)}) - \frac{\sqrt{3}}{4}\beta_1 e^{-2\pi i/3(k_1-k_2)} + \frac{\sqrt{3}}{4}\beta_3 e^{-2\pi i/3(k_1+2k_2)},$$

$$B_{13}(\mathbf{k}) = B_{31}(\mathbf{k}) = 0,$$

$$B_{22}(\mathbf{k}) = -\frac{1}{4}(\alpha_1 + \alpha_1')(e^{-2\pi i/3(k_1+2k_2)} + e^{-2\pi i/3(k_1-k_2)}) - \alpha_1' e^{2\pi i/3(2k_1+k_2)} - \frac{1}{4}\beta_1 e^{-2\pi i/3(k_1-k_2)} - \beta_1 e^{2\pi i/3(2k_1+k_2)} - \frac{1}{4}\beta_3 e^{-2\pi i/3(k_1+2k_2)},$$

$$B_{23}(\mathbf{k}) = B_{32}(\mathbf{k}) = 0,$$

$$B_{33}(\mathbf{k}) = -\alpha_1'(e^{-2\pi i/3(k_1+2k_2)} + e^{-2\pi i/3(k_1-k_2)} + e^{2\pi i/3(2k_1+k_2)}) - \beta_1 e^{-2\pi i/3(k_1-k_2)} + \beta_1 e^{-2\pi i/3(2k_1+k_2)} - \beta_3 e^{-2\pi i/3(k_1+2k_2)},$$

$$C_{11}(\mathbf{k}) = C_{22}(\mathbf{k}) = -2\alpha_f' \cos(\pi k_3),$$

$$C_{33}(\mathbf{k}) = -2\alpha_f \cos(\pi k_3),$$

$$C_{ij}(\mathbf{k}) = 0 \quad \text{if } i \neq j,$$

$$D_{11}(\mathbf{k}) = \frac{3}{2}(\alpha_1 + \alpha_1') + 3\alpha_2\left\{1 - \frac{1}{2}[\cos(2\pi k_1) + \cos 2\pi(k_1+k_2)]\right\} + \frac{3}{4}(\beta_1 + \beta_3) + \alpha_2'\left\{3 - 2\cos 2\pi k_2 - \frac{1}{2}[\cos 2\pi k_1 + \cos 2\pi(k_1+k_2)]\right\},$$

$$D_{12}(\mathbf{k}) = D_{21}(\mathbf{k}) = -\frac{\sqrt{3}}{2}\alpha_2[\cos 2\pi(k_1+k_2) - \cos(2\pi k_1)] + \frac{\sqrt{3}}{4}(\beta_1 - \beta_3),$$

$$D_{13}(\mathbf{k}) = D_{31}(\mathbf{k}) = 0,$$

$$D_{22}(\mathbf{k}) = \frac{3}{2}(\alpha_1 + \alpha_1') + 3\alpha_2\left\{1 - \frac{2}{3}\cos(2\pi k_2) - \frac{1}{6}[\cos(2\pi k_1) + \cos 2\pi(k_1+k_2)]\right\} + \frac{5}{4}\beta_1 + \frac{1}{4}\beta_3 + \alpha_2'\left\{3 - \frac{3}{2}[\cos 2\pi k_1 + \cos 2\pi(k_1+k_2)]\right\},$$

$$D_{23}(\mathbf{k}) = D_{32}(\mathbf{k}) = 0,$$

$$D_{33}(\mathbf{k}) = 3\alpha_1' + 2\beta_1 + \beta_3 + \alpha_2'\{6 - 2[\cos 2\pi k_1 + \cos 2\pi(k_1+k_2) + \cos 2\pi k_2]\},$$

$$O_{ij}(\mathbf{k}) = 0.$$

APPENDIX B: ELASTIC CONSTANTS

When we limit ourselves to graphene, the physical system is two dimensional. Using Nye's notation[36] which allows us to write the tensor relationships using more comprehensible matrices, we obtain the following relation between the strains d_i and the stresses σ_i:

$$\begin{pmatrix} \sigma_1 \\ \sigma_2 \\ \sigma_3 \end{pmatrix} = \begin{pmatrix} C_{11} & C_{12} & 0 \\ C_{12} & C_{11} & 0 \\ 0 & 0 & C_{66} \end{pmatrix} \begin{pmatrix} d_1 \\ d_2 \\ d_3 \end{pmatrix}. \tag{B1}$$

The elastic tensor is defined by only two elastic stiffness constants or moduli of elasticity $C_{ij}[C_{66} = (C_{11} - C_{12})/2]$.

Upon applying uniaxial compression or traction σ parallel to the tubule axis, if $\mathbf{R}_i$ and $\mathbf{R}_i'$ are the atomic positions before and after applying stress, then,

$$\mathbf{R}_i' = (\underline{I} + \underline{\epsilon})\mathbf{R}_i,$$

where I is the identity matrix and $\underline{\epsilon}$ the reduced deformation tensor and

$$\underline{\epsilon}_{\text{armchair}} = \begin{pmatrix} S_{12}\sigma & 0 & 0 \\ 0 & S_{11}\sigma & 0 \\ 0 & 0 & 0 \end{pmatrix}, \tag{B2}$$

$$\underline{\epsilon}_{\text{zigzag}} = \begin{pmatrix} S_{11}\sigma & 0 & 0 \\ 0 & S_{12}\sigma & 0 \\ 0 & 0 & 0 \end{pmatrix}. \tag{B3}$$

The S_{ij}'s are called elastic compliance constants or elastic constants $[S_{66}=(S_{11}-S_{12})/2]$. These two last relationships illustrate the interest,[26,27] in the case of the nanotubes, in knowing the constants S_{ij} or C_{ij} in particular C_{11} and C_{12}.

By considering the forces[29] acting on an element of volume in the crystal we obtain the equation of motion in the $O\mathbf{e}_1$ direction

$$\rho \frac{\partial^2}{\partial t^2} d_1 = C_{11}\frac{\partial^2 d_1}{\partial x^2} + C_{66}\frac{\partial^2 d_1}{\partial y^2} + (C_{12}+C_{66})\frac{\partial^2 d_2}{\partial x \partial y} \tag{B4}$$

and equivalent formulas along $O\mathbf{e}_2$ and $O\mathbf{e}_3$; ρ is the volumic mass. Taking for $\mathbf{d}$, as a plane wave propagating in the direction $\mathbf{k}$: $\mathbf{d}=\mathbf{A}e^{i(\varpi t-\mathbf{k}\cdot\mathbf{r})}$ the preceding relation yields

$$\rho\omega^2 A_1 = (C_{11}k_1^2 + C_{66}k_2^2)A_1 + (C_{12}+C_{66})k_1 k_2 A_2 . \tag{B5}$$

Identical relations exist for the other two directions so that a system of equations is obtained with nonzero solution only if the following determinant is set equal to zero:

$$\begin{vmatrix} C_{11}k_1^2 + C_{66}k_2^2 - \rho\omega^2 & (C_{12}+C_{66})k_1 k_2 \\ (C_{12}+C_{66})k_1 k_2 & C_{66}k_1^2 + C_{11}k_2^2 - \rho\omega^2 \end{vmatrix} = 0. \tag{B6}$$

In the case of a wave, longitudinally polarized in the direction $O\mathbf{e}_1$ $(A_1=A, A_2=A_3=0)$ and propagating in the direction [100] in other words $k_1=k$ and $k_2=k_3=0$ one obtains

$$C_{11[100]} = \rho\frac{\omega_L^2}{k_1^2}. \tag{B7}$$

For a wave polarized transversely along the axis $O\mathbf{e}_2$ $(A_2=A, A_1=A_3=0)$:

$$C_{66[100]} = \rho\frac{\omega_T^2}{k_1^2} \tag{B8}$$

with $\rho = 2.26\times 10^3$ kg/m^3, $\|\mathbf{k}_1\| = 4\pi/a\sqrt{3}$ and $\|\mathbf{k}_3\| = 2\pi/c$. These equations were used to evaluate the values given for nanotubes.

[1] S. Iijima, Nature (London) **354**, 56 (1991).
[2] N. Hamada, S. Sawada, and O. Oshiyama, Phys. Rev. Lett. **68**, 1579 (1992).
[3] R. Saito, M. Fujita, G. Dresselhaus, and M. Dresselhaus, Phys. Rev. B **46**, 1804 (1992).
[4] J. W. Mintmire, B. I. Dunlap, and C. T. White, Phys. Rev. Lett. **68**, 631 (1992).
[5] K. Tanaka, K. Okahara, M. Okada, and T. Yamabe, Chem. Phys. Lett. **191**, 469 (1992).
[6] M. S. Dresselhaus, G. Dresselhaus, and R. Saito, Carbon **13**, 883 (1995).
[7] K. Tanaka, H. Aoki, H. Ago, T. Yamabe, and K. Okahara, Carbon **35**, 121 (1997).
[8] Y. Saito, M. Okuda, and T. Koyama, Surf. Rev. Lett. **3**, 863 (1996).
[9] H. Ajiki and T. Ando, J. Phys. Soc. Jpn. **62**, 1255 (1993).
[10] P. C. Eklund, J. M. Holden, and R. A. Jishi, Carbon **33**, 959 (1995).
[11] J. W. Mintmire and C. T. White, Carbon **33**, 893 (1995).
[12] R. A. Jishi, D. Inomata, K. Nakao, M. S. Dresselhaus, and G. Dresselhaus, J. Phys. Soc. Jpn. **63**, 2252 (1994).
[13] J. Yu, R. K. Kalia, and P. Vashista, J. Chem. Phys. **103**, 6697 (1995).
[14] H. Hiura, T. W. Ebbesen, K. Tanigaki, and H. Takahashi, Chem. Phys. Lett. **202**, 509 (1993).
[15] N. Chandrabhas *et al.*, Pramana, J. Phys. **42**, 375 (1994).
[16] P. V. Huong, R. Cavagnat, P. M. Ajayan, and O. Stephan, Phys. Rev. B **51**, 10 048 (1995).
[17] W. S. Bacsa, D. Ugarte, A. Châtelain, and W. A. de Heer, Phys. Rev. B **50**, 15 473 (1994).
[18] J. Kastner *et al.*, Chem. Phys. Lett. **221**, 53 (1994).
[19] J. M. Holden *et al.*, Chem. Phys. Lett. **220**, 186 (1994).
[20] A. M. Rao, E. Richter, S. Bandow, B. Chase, P. C. Ecklund, K. A. Williams, S. Fang, K. R. Subbaswamy, M. Menon, A. Thess, R. E. Smalley, G. Dresselhaus, and M. S. Dresselhaus, Science **275**, 187 (1997).
[21] A. Kasuya, Y. Sasaki, Y. Saito, K. Tohji, and Y. Nishina, Phys. Rev. Lett. **78**, 4434 (1997).
[22] A. Kasuya, Y. Saito, Y. Sasaki, M. Fukushima, T. Maeda, C. Horie, and Y. Nishina, Mater. Sci. Eng. A **217/218**, 46 (1996).
[23] M. S. Dresselhaus, G. Dresselhaus, and P. C. Ecklund, *Science of Fullerenes and Carbon Nanotubes* (Academic, New York, 1996).
[24] R. A. Jishi, L. Venkataraman, M. S. Dresselhaus, and G. Dresselhaus, Chem. Phys. Lett. **209**, 77 (1993).
[25] M. Menon, E. Richter, and K. R. Subbaswamy, J. Chem. Phys. **104**, 5875 (1996).
[26] R. Heyd, A. Charlier, and E. McRae, Phys. Rev. B **55**, 6820 (1997).
[27] R. Heyd, A. Charlier, E. McRae, and M. F. Charlier, Phys. Rev. B **56**, 9958 (1997).
[28] J. De Launay, Solid State Phys. **3**, 203 (1957).
[29] L. Lang, S. Doyen-Lang, A. Charlier, and M. F. Charlier, Phys. Rev. B **49**, 5672 (1994).
[30] D. J. Klein, W. A. Seitz, and T. G. Schmalz, J. Phys. Chem. **97**, 1231 (1993).

[31] L. J. Raubenheimer and G. Gilat, Phys. Rev. **157**, B586 (1967).
[32] A. P. P. Nicholson and D. J. Bacon, J. Phys. C **10**, 2295 (1977).
[33] K. K. Mani and R. Ramani, Status Solidi **61**, 659 (1974).
[34] R. Niclow, N. Wakabayashi, and H. G. Smith, Phys. Rev. B **5**, 4951 (1972).
[35] L. Landau and E. Lifchitz, *Théorie de l Élasticité* (Editions Mir, Moscou, 1967).
[36] J. F. Nye, *Physical Properties of Crystals* (Clarendon Press, Oxford, 1985).